USAFA-TR-76-20

GPS SPIN PHASE DYNAMICS AND SPIN-DOWN ANALYSIS

MAJOR ROGER P. NEELAND

DEPARTMENT OF ASTRONAUTICS
AND
COMPUTER SCIENCE
USAF ACADEMY, COLORADO 80840

SEPTEMBER 1976

FINAL REPORT

Prepared for

USAF SPACE AND MISSILE SYSTEMS ORGANIZATION
DEPUTY FOR SPACE NAVIGATION SYSTEMS
LOS ANGELES, CA 90009

DEAN OF THE FACULTY
UNITED STATES AIR FORCE ACADEMY
COLORADO 80840

UNCLASSIFIED

SECURITY CLASSIFICATION OF THIS PAGE *(When Data Entered)*

REPORT DOCUMENTATION PAGE		READ INSTRUCTIONS BEFORE COMPLETING FORM
1. REPORT NUMBER USAFA-TR-76-	2. GOVT ACCESSION NO.	3. RECIPIENT'S CATALOG NUMBER
4. TITLE *(and Subtitle)* GPS SPIN PHASE DYNAMICS AND SPINDOWN ANALYSIS		5. TYPE OF REPORT & PERIOD COVERED Final Report 6. PERFORMING ORG. REPORT NUMBER USAFA-TR-76-20
7. AUTHOR(s) Roger P. Neeland		8. CONTRACT OR GRANT NUMBER(s) SAMSO/YE Project Order 76-1
9. PERFORMING ORGANIZATION NAME AND ADDRESS Department of Astronautics and Computer Science (DFACS) US Air Force Academy, CO 80840		10. PROGRAM ELEMENT, PROJECT, TASK AREA & WORK UNIT NUMBERS
11. CONTROLLING OFFICE NAME AND ADDRESS Dean of Faculty, USAF Academy, CO 80840 SAMSO/YE, Los Angeles AFS, CA 90009		12. REPORT DATE September 1976 13. NUMBER OF PAGES
14. MONITORING AGENCY NAME & ADDRESS*(if different from Controlling Office)*		15. SECURITY CLASS. *(of this report)* Unclassified 15a. DECLASSIFICATION/DOWNGRADING SCHEDULE

16. DISTRIBUTION STATEMENT *(of this Report)*

Approved for public release; distribution unlimited

17. DISTRIBUTION STATEMENT *(of the abstract entered in Block 20, if different from Report)*

18. SUPPLEMENTARY NOTES

19. KEY WORDS *(Continue on reverse side if necessary and identify by block number)*

Global Positioning System (GPS)
Spacecraft Dynamics
Satellite Attitude Control
Digital Computer Simulation of Spacecraft Dynamics

20. ABSTRACT *(Continue on reverse side if necessary and identify by block number)*

The NAVSTAR/GPS NDS-2 satellite will be spin stabilized at approximately 100 revolutions per minute during its early flight phases, but must be nearly motionless relative to its orbit and pointing at the earth during its operational lifetime. Present plans call for the despin to be accomplished in several phases, allowing the nutation damper on the satellite to remove any nutation caused during the thrusting despin phase. This study

DD FORM 1 JAN 73 1473 EDITION OF 1 NOV 65 IS OBSOLETE

UNCLASSIFIED

SECURITY CLASSIFICATION OF THIS PAGE *(When Data Entered)*

20. investigates several aspects of the despin operation, including probable magnitudes of error torques due to thrust misalignment. Extensive computer simulations have verified a simplified analytic model of satellite behavior which gives insight into the expected behavior of a spinning, non-symmetric body. Insight is developed into the behavior of this type body, subject to random error torques and intentional despin torques. The extremely slow spin range of 6 to 1 revolution per minute is examined, and the consequences of stopping and starting despin thrust at an intermediate speed is found to be undesirable in a "worst possible case" sense.

Editorial Review by Lt. Colonel Jack M. Shuttleworth
Department of English and Fine Arts
USAF Academy, Colorado 80840

This research report is presented as a competent treatment of the subject, worthy of publication. The United States Air Force Academy vouches for the quality of the research, without necessarily endorsing the opinions and conclusions of the author.

This report has been cleared for open publication and/or public release by the SAMSO Office of Information in accordance with AFR 190-17 and DODD 5230.9. There is no objection to unlimited distribution of this report to the public at large, or by DDC to the National Technical Information Service.

This research report has been reviewed and is approved for publication.

/ Philip J. Erdle

PHILIP J. ERDLE, Colonel, USAF
Vice Dean of the Faculty

Additional copies of this document are available through the National Technical Information Service, U.S. Department of Commerce, 5285 Port Royal Road, Springfield, VA 22151.

TABLE OF CONTENTS

I. INTRODUCTION

The NAVSTAR/GPS NDS-2 satellite will be spin stabilized at approximately 100 revolutions per minute during its early flight phases, but must be nearly motionless relative to its orbit and pointing toward the earth during its operational lifetime. Present plans call for the despin to be accomplished in several phases allowing the nutation damper to remove any nutational motion caused by thruster misalignment during the despin periods. This report covers portions of the USAFA Independent Stability and Control Analysis performed during June and July 1976 on the dynamic behavior of the satellite during this spindown prior to earth acquisition. Most results presented are analytic, with results of digital simulation included to verify the analytic work. The last two sections discuss simulated behavior not predicted by the analytic results, and give heuristic explanations for this behavior. Some detailed derivations and simulation summaries are given in appendices.

II. BACKGROUND, TERMINOLOGY, AND ASSUMPTIONS

The behavior of a non-symmetric body spinning about the z axis can be represented by Euler's equations. Using principal body axes these equations are

$$I_x \dot{\omega}_x + (I_z - I_y)\, \omega_y \omega_z = M_x \tag{2-1}$$

$$I_y \dot{\omega}_y + (I_x - I_z)\, \omega_x \omega_z = M_y \tag{2-2}$$

$$I_z \dot{\omega}_z + (I_y - I_x)\, \omega_x \omega_y = M_z \tag{2-3}$$

ω_x, ω_y and ω_z are the respective inertial angular rates in the principal axis frame; I_x, I_y and I_z are moments of inertia about the principal axes; M_x, M_y, M_z are respective body axis torques. The principal angle of interest in this study, nutation angle, is defined in terms of principal spin axis and tangential angular momenta as

$$\tan \nu(t) \doteq \frac{H_T(t)}{H_z(t)} = \frac{\sqrt{(I_x\omega_x)^2 + (I_y\omega_y)^2}}{I_z\omega_z} \tag{2-4}$$

where the principal spin axis is the z body axis. In all derivations, we assume $\nu(t)$ is a small angle, i.e.

$$\tan \nu(t) \cong \nu(t) = \frac{H_T(t)}{H_z(t)} \tag{2-5}$$

The explicit use of t as an argument of functions is dropped where possible in the interests of brevity. We also assume that I_x and I_y are nearly equal, i.e.

$$(I_y - I_x) \doteq \Delta I << I_z \tag{2-6}$$

In addition, the small angle assumption for ν implies $I_x\omega_x << I_z\omega_z$ and $I_y\omega_y << I_z\omega_z$. For GPS $\frac{I_x}{I_z} \approx \frac{I_y}{I_z} \approx .9$, so $\omega_x << \omega_z$ and $\omega_y << \omega_z$.

The previous two assumptions, together with (2-3), allow us to infer that in the absence of torque about the z axis, M_z,

$$\dot{\omega}_z \approx 0 \text{ or } \omega_z(t) = \text{constant} = \omega_{z_o} \tag{2-7}$$

Looking again at the unforced case, we see that if I_z is the maximum inertia, and we are spinning in the positive sense about the z axis, then

$$\omega_x > 0 \Rightarrow \dot{\omega}_y > 0 \tag{2-8}$$

$$\omega_y > 0 \Rightarrow \dot{\omega}_x < 0 \tag{2-9}$$

or, as shown graphically in Figure 2-1, we expect the following precession of the tangential (non-spin) angular momentum.

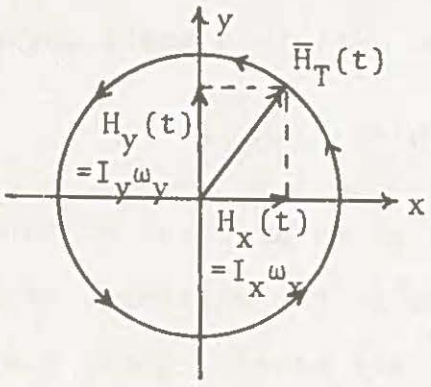

Figure 2-1

Natural Precession of Tangential Angular Momentum

This simple and perhaps elementary fact is quite useful in interpreting and specifying consistent initial conditions for simulations.

III. NATURAL BEHAVIOR OF NUTATION ANGLE

In terms of body angular rates and using the previous assumptions, we may derive the equation of motion for transverse angular momentum and nutation angle (see Appendix A):

$$\dot{H}_T = \frac{H_z}{H_T}\left[\omega_x\omega_y\Delta I + \frac{H_x}{H_z}M_x + \frac{H_y}{H_z}M_y\right] \tag{3-1}$$

$$\dot{\nu} = \frac{\omega_x\omega_y}{H_T}\Delta I + \frac{1}{H_T}\left[\frac{H_x}{H_z}M_x + \frac{H_y}{H_z}M_y - \nu^2 M_z\right] \tag{3-2}$$

In general, these equations are difficult to integrate analytically, but some special cases are enlightening. In particular, we first examine the unforced natural response of the system. By letting all torques be zero, we are neglecting the effect of a nutation damper as well as jet torques. Equations 2-1 and 2-2 have been solved by various authors [2,3] under these assumptions with the result that in most general form

$$\omega_y(t) = A_y \cos \omega_n t + B_y \sin \omega_n t \tag{3-3}$$

$$\omega_x(t) = A_x \cos \omega_n t + B_x \sin \omega_n t \tag{3-4}$$

where

$$\omega_n \doteq \sqrt{\frac{(I_z - I_x)(I_z - I_y)}{I_x I_y}}\,\omega_z \doteq K_1\omega_z \tag{3-5}$$

For GPS/NDS with solar panels in, during spindown, $K_1 \cong .13$. We expect then the basic motion of ω_x and ω_y to have a period

about 7.6 times the period of rotation. Simulation runs confirmed this type behavior.

We may obtain relatively simple expressions for $\omega_x(t)$ and $\omega_y(t)$, by defining the initial time of our simulation and t = 0 of our analytic expressions to correspond to the point on Figure 2-1 at which $\omega_x(0) = 0$ and $\omega_y(0) = \omega_{y_{max}} \doteq \omega_{y_o}$. Letting

$$H_{T_o} \doteq H_T(0) \equiv I_y \omega_{y_o} \tag{3-6}$$

we have (see Appendix A)

$$\omega_y(t) = \frac{H_{T_o}}{I_y} \cos \omega_n t \tag{3-7}$$

$$\omega_x(t) = -\frac{H_{T_o}}{I_y} K_2 \sin \omega_n t \tag{3-8}$$

where

$$K_2 \doteq \sqrt{\left(\frac{I_y}{I_x}\right)\left(\frac{I_z - I_y}{I_z - I_x}\right)} \tag{3-9}$$

We note that if $I_x = I_y$ we will have $K_2 = 1$. K_2 is approximately 0.7 during the spindown phase for GPS, in which case we note that ω_x oscillates between smaller maximum values than ω_y. This behavior was also verified by the simulation. If we now put these expressions in Equation 3-2, we obtain (see Appendix A)

$$\nu(t) = \nu_o \sqrt{1 + K_3(\cos 2\omega_n t - 1)} \qquad (3\text{-}10)$$

where

$$K_3 = \frac{1}{2} \frac{\Delta I}{I_z - I_x} \left(\frac{I_z}{I_y}\right) \qquad (3\text{-}11)$$

and

$$\nu_o \doteq \nu(0) \qquad (3\text{-}12)$$

(Note that if $\Delta I = 0$, $\nu(t)$ will remain constant, i.e. spin is about the principal spin axis.) Simulations verified the results of Equation 3-10. We may also note that $\nu_{minimum}$ occurs when $\omega_n t = 90^o$, 270^o, ..., at which time

$$\nu_{min} = \nu\left(\frac{j\pi}{2\omega_n}\right) = \frac{I_x}{I_y} K_2 \nu_o \qquad j = 1,3,5,... \qquad (3\text{-}14)$$

These computations are useful in that they allow us to isolate the behavior of $\nu(t)$ due only to the asymmetry of the body, and to focus on those effects due to torques such as the nutation damper, thruster misalignments, and intentional despin torques.

IV. FORCED BEHAVIOR OF NUTATION ANGLE

The integration of Equation 3-2, including the effects of forcing torques, is extremely difficult, even under the simplifying assumptions already made. We may make only general observations. Let us predict system behavior as $\Delta I \to 0$, (we approach a body of revolution.) Under this most stringent constraint we can show that if we are despinning about the z axis and have no torques other than about the z axis, we expect

$$\nu(t) = \left(\frac{\omega_{z_o}}{\omega_z(t)}\right)\nu_o \qquad (4\text{-}1)$$

This behavior is due only to the fact that $H_z(t)$ is being reduced while $H_T(t)$ is not (under these assumptions). This model describes the "mean" behavior of $\nu(t)$ during spindown surprisingly well, but tends to overestimate the growth of $\nu(t)$ as time progresses. It is, however, useful as a rough guide. One effect for which this mode does not account is that, for $\Delta I \neq 0$, at the time despin firing stops, the nutation angle (as presented in Equation 3-10) may not be at its natural maximum. As a result, we in fact notice $\nu(t)$ increasing even after despin firing stops, sometimes up to approximately $1/K_2$ times its value at the time of thrust termination.

Another effect quite noticeable in simulations is the sensitivity of final nutation angle to the time of firing

when error torques (such as thrust misalignment) are present. This sensitivity should be anticipated from Equation 3-2. We note that M_x and M_y may increase or decrease the nutation angle, depending on the signs of the torques and the phase of the precession (signs of H_x and H_y). Since the signs and magnitudes of M_x and M_y are by definition unknown random constants (see Appendix B), it is not possible to choose the "best" time to fire for despin, even if precession phase were measurable, which it is not for GPS/NDS. Since the forced behavior predicted in Equation 4-1 is dependent on ν_o at time of firing, and this in turn is dependent on the unmeasured precession phase angle during unforced rotation, we have an additional random element introduced. With additional instrumentation such as rate gyros, it would theoretically be possible to estimate the thruster misalignments, as they are unknown but constant.

Two effects could be seen during despin. One increase in ν was a nearly linear function of ν_o. Equations 4-1 and 3-10 summarize this effect. The other increase in ν was independent of ν_o and was the effect of misalignment torques M_x and M_y. The increase in ν during a thrust period was nearly linear in its reaction to these torques. The two effects cannot always be directly added because they may not be "in phase."

V. NUMERICAL RESULTS OF SPINDOWN SIMULATIONS

Extensive simulation runs of spindown operations from 20 rpm down to 1 rpm were made with various thrust misalignments. No major problems were encountered down to 6 rpm, as the nutation damper is reasonably effective down to this speed, and any nutation angle built up is dissipated before starting the next step of spindown.

The most comprehensive runs involved the region below 6 rpm. Error torques simulated corresponded to misalignment angles of 0, 1, and 2 degrees. As expected, the larger error torques gave the more extreme behavior. Simulations were made starting with $.5^{o}$ nutation angle at 6 rpm and despinning to 2 rpm - then starting the spindown to 1 rpm at several different times in the precessional cycle, starting from the natural motion existing at the end of spindown to 2 rpm. Another set of runs with the same range of thrust misalignment errors was made spinning down directly from 6 to 1 rpm. This will be referred to as the one-step approach. Although not a complete sampling of all firing times and error misalignments, Figure 5-1 summarizes the range of results obtained:

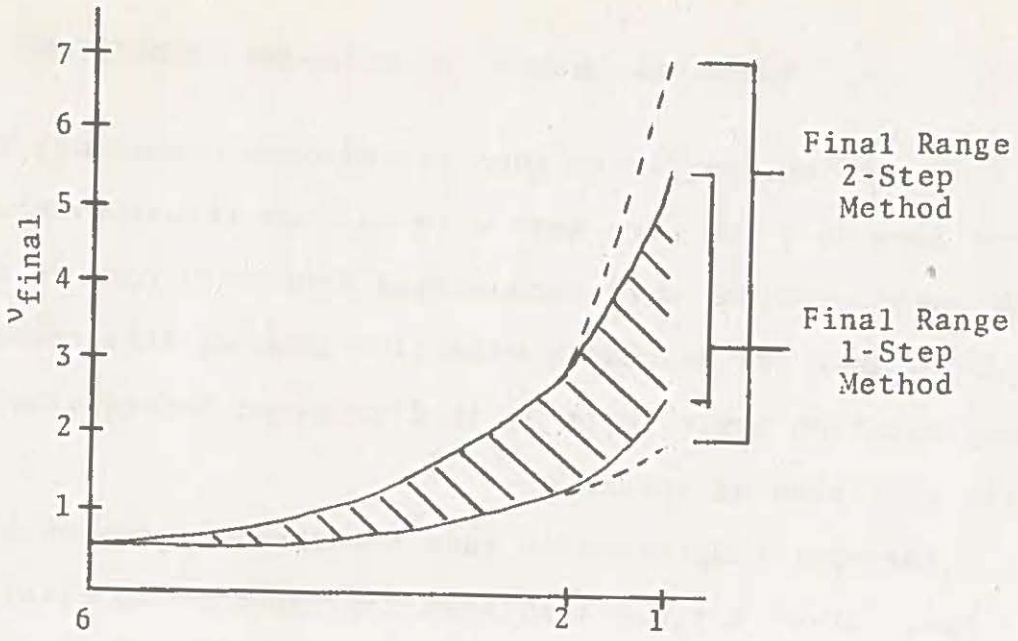

Figure 5-1

Results of Low-speed Spindown Simulation

The exact numbers for final nutation angle at various speeds might be different with a statistically significant sample, but the general shape and relative positions of the final nutation angle ranges should remain the same.

VI. RECOMMENDATIONS AND CONCLUSIONS

Simulation results, based on thruster torques due to misalignment of 2^{o} or less, indicate that most nutational behavior will be of the type discussed under natural behavior and behavior due to intentional despin torque. At any spin rate, but noticeably at low speeds, the effect of misalignment torques may be either stabilizing or destabilizing and is unpredictable in both magnitude and sign unless further instrumentation is added to the present system. This should be considered for future missions.

The following conclusions are drawn from simulations summarized in Section V and specifically address the question of whether it is advantageous to stop the despin process at 2 rpm and then proceed to 1 rpm. Firstly, in a probabilistic (mean value) sense, there is no advantage to stopping at 2 rpm, assuming that the nutation damper has negligible effect at this speed. The time constant of the damper effect is on the order of several hours theoretically. Secondly, the worst and best nutation angle resulting from a plan stopping at 2 rpm would be larger and smaller respectively than if despin was continued directly from 6 to 1 rpm. If the management criterion is to minimize the maximum nutation angle rather than the expected angle, it would appear better to despin directly from 6 to 1 rpm. Under the assumption that we have no nutation at 6 rpm, we should still expect 2^{o}

to 3^{o} nutation at 1 rpm, no matter how we despin, if we have approximately 2^{o} thruster misalignment. This range should be recognized as an engineering judgement since the cost of simulating sufficient combinations of firing times and misalignment angles to make a valid statistical statement is prohibitive.

REFERENCES

1. Parkinson, B.W. "Closed Form Solution for Motion of a Spinning Rigid Body." AIAA Journal of Spacecraft and Rockets 5 (May 1968): 606-607.

2. Thompson, W.T. Introduction to Space Dynamics. New York: Wiley and Sons, Inc., 1963.

3. Wrigley, Walter; Hollister, Walter; and Denhard, William. Gyroscopic Theory, Design, and Instrumentation. Cambridge, MA: MIT Press, 1969.

APPENDIX A

DERIVATION OF DYNAMIC EQUATIONS

APPENDIX A

DERIVATION OF DYNAMIC EQUATIONS

Given:

$$H_T \doteq \left[\left(I_x\omega_x\right)^2 + \left(I_y\omega_y\right)^2\right]^{\frac{1}{2}} \tag{A-1}$$

$$\frac{d}{dt} H_T = \frac{1}{H_T}\left[I_x{}^2\omega_x\dot{\omega}_x + I_y{}^2\omega_y\dot{\omega}_y\right] \tag{A-2}$$

Using Euler's equations 2-1 through 2-3

$$\frac{d}{dt} H_T = \frac{1}{H_T}\left[\omega_x\omega_y\omega_z I_z\Delta I + \omega_x M_x I_x + \omega_y M_y I_y\right] \tag{A-3}$$

To derive the nutation angle equation, we assume that ω_z is constant except for the change caused by M_z.

$$\frac{d\nu}{dt} = \frac{d}{dt}\left(\frac{H_T}{H_z}\right) = \frac{H_z\dot{H}_T - \dot{H}_z H_T}{H_z{}^2} \tag{A-4}$$

$$\frac{d\nu}{dt} = \frac{1}{H_z H_T}\left[(\omega_x\omega_y\omega_z I_z\Delta I) + H_x M_x + H_y M_y\right] - \frac{M_z H_T}{H_z{}^2} \tag{A-5}$$

$$\frac{d\nu}{dt} = \frac{\omega_x\omega_y}{H_T}\Delta I + \frac{1}{H_T}\left[\frac{H_x M_x}{H_z} + \frac{H_y M_y}{H_z} - \left(\frac{H_T}{H_z}\right)^2 M_z\right] \tag{A-6}$$

Starting from the result that for ω_z constant and no torques, ω_x and ω_y behave as a second order system with natural frequency $\omega_n = K_1\omega_z$ (Reference 3). We have

$$\omega_y(t) = A_y \cos\omega_n t + B_y \sin\omega_n t \tag{A-7}$$

$$\dot{\omega}_y(t) = -A_y\omega_n \sin \omega_n t + B_y\omega_n \cos \omega_n t \qquad \text{(A-8)}$$

$$\omega_x(t) = A_x \cos \omega_n t + B_x \sin \omega_n t \qquad \text{(A-9)}$$

$$\dot{\omega}_x(t) = -A_x\omega_n \sin \omega_n t + B_x\omega_n \cos \omega_n t \qquad \text{(A-10)}$$

We define the time t = 0 such that

$$\omega_y(0) = \omega_{y_o} \qquad \text{(A-11)}$$

$$\omega_x(0) = 0 \qquad \text{(A-12)}$$

Which implies from the Euler equations

$$\dot{\omega}_y(0) = 0 \qquad \text{(A-13)}$$

$$\dot{\omega}_x(0) = -\left(\frac{I_z - I_y}{I_x}\right)\omega_z\omega_{y_o} \qquad \text{(A-14)}$$

Substituting A-11 and A-13 in A-7 and A-8 gives

$$B_y = 0 \qquad \text{(A-15)}$$

$$A_y = \omega_{y_o} \qquad \text{(A-16)}$$

Substituting A-12 and A-14 in A-9 and A-10 gives

$$A_x = 0 \qquad \text{(A-17)}$$

$$B_x = \frac{-\omega_{y_o}}{K_1}\left(\frac{I_z - I_y}{I_x}\right) \qquad \text{(A-18)}$$

Using the definition of K_1

$$B_x = -\omega_{y_o}\left(\frac{I_z - I_y}{I_x}\right)\sqrt{\frac{I_xI_y}{(I_z-I_x)(I_z-I_y)}} = -\omega_{y_o}\sqrt{\frac{I_y(I_z-I_y)}{I_x(I_z-I_x)}} \qquad \text{(A-19)}$$

Therefore,

$$\omega_y(t) = \omega_{y_o} \cos \omega_n t \tag{A-20}$$

$$\omega_x(t) = -\omega_{y_o} K_2 \sin \omega_n t \tag{A-21}$$

where K_2 is defined by Equation A-19.

With this convenient form for ω_x and ω_y, it is relatively straightforward to integrate the unforced special cases of Equations A-3 and A-6. Since they are essentially the same equations, we will integrate only Equation A-6.

$$\frac{d\nu}{dt} = \frac{-\Delta I}{H_T} \omega_{y_o}^2 K_2 \cos \omega_n t \sin \omega_n t \tag{A-22}$$

$$= \frac{-\Delta I \ \omega_{y_o}^2 \ K_2}{2H_T} \sin 2\omega_n t \tag{A-23}$$

$$= \left(\frac{-\Delta I}{4H_T}\right)\left(\frac{K_2}{K_1}\right) \frac{\omega_{y_o}^2}{\omega_z} \ 2\omega_n \ \sin 2\omega_n t \tag{A-24}$$

$$= -\frac{1}{4} \left(\frac{I_z \omega_z}{H_T}\right)\left(\frac{I_y \ \omega_{y_o}}{I_z \ \omega_z}\right)^2 \left(\frac{I_z \ \Delta I \ K_2}{I_y^2 \ K_1}\right) 2\omega_n \ \sin 2\omega_n t \tag{A-25}$$

$$= -\frac{\nu_o^2}{2\nu} \left[\frac{I_z \ \Delta I \ K_2}{2I_y^2 \ K_1}\right] 2\omega_n \ \sin 2\omega_n t \tag{A-26}$$

The bracketed term involving inertias may be reduced to the simple form

$$K_3 = \frac{\Delta I}{2} \left(\frac{I_z K_2}{I_y^2 K_1}\right) = \frac{1}{2} \left(\frac{\Delta I}{I_z - I_x}\right)\left(\frac{I_z}{I_y}\right) \tag{A-27}$$

so that

$$v dv = -\frac{v_o^2}{2} K_3 \sin 2\omega_n \quad (2\omega_n t) dt \qquad \text{(A-28)}$$

Integrating we obtain

$$\frac{v^2}{2} = \frac{v_o^2}{2} K_3 \cos 2\omega_n t + C_o \qquad \text{(A-29)}$$

where

$$C_o = \frac{v_o^2}{2} (1 - K_3) \qquad \text{(A-30)}$$

giving

$$v(t) = v_o \sqrt{1 + K_3(\cos 2\omega_n t - 1)} \qquad \text{(A-31)}$$

APPENDIX B

DERIVATION OF ERROR TORQUES

APPENDIX B

DERIVATION OF ERROR TORQUES

This section develops the methods used to determine error torques. We assume the use of two opposed thrusters (nominally 12 and 14) which provide torque about the negative z axis to effect spindown. They are positioned with respect to the center of mass as shown in Figure B-1.

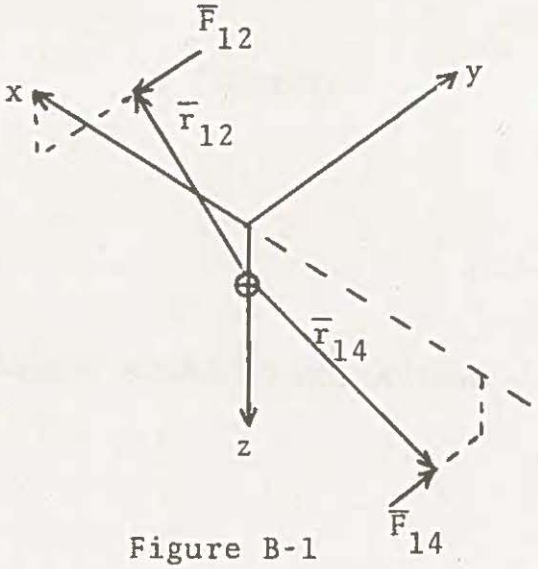

Figure B-1
Geometry of Thrusters

Looking in detail at thruster 12, we can define misalignment angles in the x,y and y,z planes as shown in Figures B-2 and B-3.

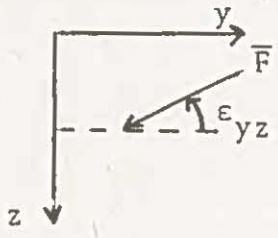

Figure B-2
Definition of ε_{yz}

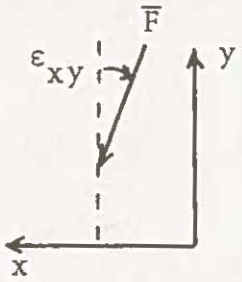

Figure B-3
Definition of ε_{xy}

The angles ε_{yz} and ε_{xy} are defined so as to provide positive torques about the x and y axis respectively. We shall assume that the misalignment angles allow use of the "small angle approximation." We know that

$$\bar{M} = \begin{bmatrix} M_x \\ M_y \\ M_z \end{bmatrix} = \bar{r} \times \bar{F} \tag{B-1}$$

where $\bar{M}$ and $\bar{r}$ are both with respect to the body center of mass. We may compute for thruster 12

$$\bar{r}_{12} = \begin{bmatrix} r_x \\ r_y \\ r_z \end{bmatrix} \tag{B-2}$$

$$\bar{F}_{12} = Th \begin{bmatrix} \varepsilon_{xy} \\ -1 \\ \varepsilon_{yz} \end{bmatrix} \tag{B-3}$$

where Th is the thruster level. Then

$$\bar{M} = Th \begin{bmatrix} r_y\ \varepsilon_{yz} + r_z \\ r_z\ \varepsilon_{xy} - r_x\ \varepsilon_{yz} \\ -r_x\ -r_y\ \varepsilon_{xy} \end{bmatrix} \tag{B-4}$$

We may do the same for thruster 14. To keep the computations more simple, we assume the two thrusters are located symmetrically with respect to the center of mass, but this is

not necessarily true. If the thruster block were rotated, it would not be true. Using subscript 14 to denote error angles of thruster 14, which are defined analogously to thruster 12, we have

$$\bar{M}_{14} = Th \begin{bmatrix} r_y \, \varepsilon_{yz_{14}} - r_z \\ r_z \, \varepsilon_{xy_{14}} - r_x \, \varepsilon_{yz_{14}} \\ -r_x + r_y \, \varepsilon_{xy_{14}} \end{bmatrix} \tag{B-5}$$

Combining the effects of the two thrusters

$$\bar{M}_{Total} = Th \begin{bmatrix} r_y \left(\varepsilon_{yz_{12}} + \varepsilon_{yz_{14}}\right) \\ r_z \left(\varepsilon_{xy_{12}} + \varepsilon_{xy_{14}}\right) - r_x \left(\varepsilon_{yz_{12}} + \varepsilon_{yz_{14}}\right) \\ -2r_x \end{bmatrix} \tag{B-6}$$

We note that the error torques are uncertain in both direction and magnitude, varying with the thruster misalignment angles, which may be independent of each other, and possibly with uncertainty in thruster position. The misalignments could be estimated if accurate measurements of body angular rates were available. When Section V speaks of "2^o misalignment," it means that both thrusters have a positive value of 2^o in both errors.